



## Landslide Susceptibility Assessment Using Combined TRIGRS and Flow-R

Ahmad Rifa'i<sup>1\*</sup>, Ragil A. Yuniawan<sup>1,2</sup>, Fikri Faris<sup>1</sup>, Tiara R. Trisnawati<sup>1</sup>,  
Byon Rezy Pradana Purba<sup>1</sup>, Andy Subiyantoro<sup>3,4</sup>, Eka Priangga Hari Suryana<sup>2</sup>,  
Banata Wahid Ridwan<sup>2</sup>

<sup>1</sup> Department of Civil and Environmental Engineering, Faculty of Engineering, Universitas Gadjah Mada, Yogyakarta 55281, Indonesia.

<sup>2</sup> Balai Teknik Sabo, Direktorat Bina Teknik, Ministry of Public Works and Housing, Yogyakarta 55282, Indonesia.

<sup>3</sup> Faculty of Geoinformation Science and Earth Observation (ITC), University of Twente, Enschede 7514 AE, The Netherlands.

<sup>4</sup> Balai Besar Wilayah C3, Direktorat Jenderal Sumber Daya Air, Ministry of Public Works and Housing, Banten 206111, Indonesia.

Received 25 October 2024; Revised 18 January 2025; Accepted 02 February 2025; Published 01 March 2025

### Abstract

Landslides were addressed as one of the natural hazards that can create extensive disasters. Effective assessment to locate potential landslide events is crucial for planning and risk mitigation. This study, which is located in the Sumitro watershed, Kulon Progo, Yogyakarta, presents a novel approach to landslide susceptibility assessment by integrating the Transient Rainfall Infiltration and Grid-Based Regional Slope-Stability Model (TRIGRS) with the Flow-R model. Five key parameters, namely slope, soil properties, groundwater level, soil thickness, and rainfall, were used to create the landslide susceptibility zonation. TRIGRS was used to identify the landslide initiation, while Flow-R was used to create the run-out area. The result was then validated through statistical evaluation using Area Under Curve (AUC) based on the landslide inventory. Results show that landslide susceptibility zonation created from TRIGRS alone resulted in an AUC value of 0.679, while the combination of TRIGRS-Flow-R susceptibility zonation shows a better AUC value of 0.728. The increase of the AUC value of almost 0.05 has enhanced the correlation between the landslide susceptibility zonation and landslide inventory from “acceptable” to “excellent” correlation. This result demonstrates that integrating Flow-R with TRIGRS improves the performance of landslide susceptibility zonation. This study offers a new perspective on creating landslide susceptibility zonation by combining two methods, yielding more reliable results.

*Keywords:* Landslide; Landslide Susceptibility Zonation; TRIGRS; Flow-R; AUC.

## 1. Introduction

Landslides were addressed as one of the natural hazards that can create extensive disasters [1-3]. This disaster has occurred continuously in several countries, especially mountainous areas with high rainfall intensity, such as Indonesia [4]. The Indonesian government's efforts to mitigate the landslides are carried out with both physical and non-physical methods, such as slope stabilization, landslide early warning systems (LEWS), landslide susceptibility zonation, and even establishing regulations related to landslide mitigation [5]. Among those mitigation methods, creating a landslide susceptibility zonation was the most common to apply [6]. This method does not need much money and can give early information about the potential area to be affected by the landslide [7].

\* Corresponding author: [ahmad.rifai@ugm.ac.id](mailto:ahmad.rifai@ugm.ac.id)

 <http://dx.doi.org/10.28991/CEJ-2025-011-03-020>



© 2025 by the authors. Licensee C.E.J, Tehran, Iran. This article is an open access article distributed under the terms and conditions of the Creative Commons Attribution (CC-BY) license (<http://creativecommons.org/licenses/by/4.0/>).

Creating landslide susceptibility zonation remains challenging [8, 9]. Various methods have been developed to generate landslide susceptibility zonation, which can generally be categorized into heuristic, statistical, and deterministic methods [10, 11]. Heuristic or qualitative methods rely on expert judgment to assign weights to various factors contributing to landslide occurrence [12]. Examples of heuristic methods are the Analytical Hierarchy Process (AHP) and Weight of Evidence (WoE) [13-17]. Statistical methods, on the other hand, utilize historical landslide data to identify correlations between landslide occurrences and potential causative factors [11, 18]. These approaches range from simpler techniques like bivariate and multivariate regression to advanced machine learning algorithms [19, 20]. Examples of statistical methods are Frequency Ratio (FR), Logistic Regression (LR), Random Forests (RF), and Artificial Neural Networks (ANN) [17, 21-23]. Deterministic methods, particularly physically-based modeling, offer the most detailed analysis for landslide susceptibility zonation [11]. These methods simulate the physical forces acting on slopes, such as gravitational forces, soil cohesion, and pore water pressure, to calculate the Safety Factor (SF) [24]. By modeling both the driving and resisting forces, physically-based modeling provides a mechanistic understanding of landslide processes.

Every method used to establish landslide susceptibility zonation has its strengths and limitations. Heuristic methods are simple and practical, particularly in areas with limited data [25]. This method relies heavily on expert judgment, which can be highly subjective, making it better suited for preliminary assessments [12]. Statistical methods, especially when integrated with machine learning, and deterministic methods (physically-based modeling) generally exhibit higher accuracy and can effectively represent the relationships between landslide events and contributing factors [26]. Machine learning models, being data-driven, are highly dependent on the quality and quantity of landslide inventory data for training and validation [27, 28].

In contrast, the physically-based models, grounded in physical principles, require detailed geotechnical and hydrological investigations to perform accurate modeling [29]. As a result, machine learning models are better used for large-scale susceptibility assessments with good landslide inventory data but lack the data required for modeling, while the physically-based models are more suitable for smaller areas with reliable geotechnical and hydrological data. In mountainous areas where landslide inventories are poorly recorded, such as regions with tropical climates where rapid vegetation growth often obscures landslide scars, creating good landslide inventories is challenging [30, 31]. Hence, establishing landslide susceptibility zonation in small areas using physically-based models is the best option for this location.

In many cases, applying the deterministic method through a physically-based model has shown promising results [32, 33]. However, many of them focus solely on landslide susceptibility zonation without considering secondary hazards, such as debris flows, which can substantially expand the area affected by the initial landslide [32, 34, 35]. This study introduces a new approach to landslide susceptibility assessment by combining the Transient Rainfall Infiltration and Grid-Based Regional Slope-Stability Model (TRIGRS) with the Flow-R model. TRIGRS simulates the transient stability of slopes under varying rainfall conditions, providing a dynamic assessment of potential landslide initiation points [36, 37]. By incorporating the effects of rainfall infiltration on pore-water pressure, TRIGRS offers a more accurate prediction of landslide occurrences. This program has proven to give good results in mountainous areas [38]. Flow-R, on the other hand, is used to model the run-out behavior of landslides and debris flows. This model estimates the propagation and impact zones of landslides identified by TRIGRS, allowing for a comprehensive analysis of landslide initiation and debris flow pathways [39]. The integration of these two models addresses a critical gap in existing landslide susceptibility assessment, which often overlooks the complex interactions between rainfall, slope stability, and debris flow dynamics. By employing this combined approach, we aim to create a more robust and detailed landslide susceptibility zonation that identifies areas susceptible to landslides and predicts the potential extent of debris flow impact. This approach addresses the limitations of traditional landslide susceptibility zonation and offers a comprehensive tool for understanding and managing landslide risks in susceptible regions.

The structure of this article is organized as follows: Section 1 contains the introduction and background of this study. Section 2 provides an overview of the study area, while section 3 outlines the data required for the analysis. Section 4 describes the methodology, including the integration of TRIGRS and Flow-R models, as well as the validation process. Section 5 presents the results and discussion, including comparisons with previous studies. Finally, Section 6 concludes the study, highlighting key findings and offering recommendations for future research.

## 2. Study Area

The study area is located in the Sumitro Watershed, which lies in the Menoreh Mountains, Kulon Progo, Yogyakarta, Indonesia. Numerous landslides have occurred at this location, mostly when the rainfall season is coming. Apart from high rainfall intensity, steep slopes, humid climate, and dense trees are the causes of landslides in the research area. The research area covers approximately 8,510 hectares, with most of the terrain consisting of forests, plantations, and agricultural land. Refer to (Figure 1) for a visual depiction of the study area (source: <https://tanahair.indonesia.go.id> with modifications).

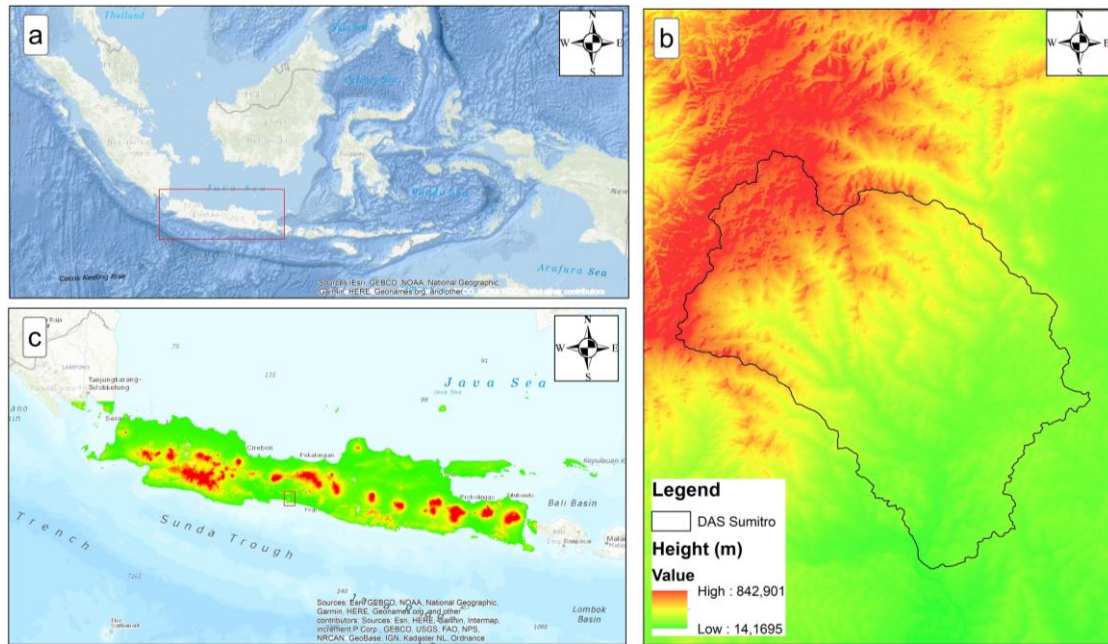


Figure 1. Study area in Sumitro Watershed

The geological setting within the research location encompasses the Jonggrangan, Kebobutak, and Sentolo formations. The Kebobutak formation, identified as Middle Miocene in age, is characterized by Sandstone, Silt, Clay, Tuff, and Agglomerate rocks. Positioned above the Kebobutak Formation, the Jonggrangan Formation consists of carbonate sandstone, granular limestone, and reef limestone. Meanwhile, the Sentolo formation, belonging to the Late Miocene-Pliocene period, comprises agglomerate, marl, and limestone. The geological structure at the research site features three normal faults: the first fault aligns in a west-east direction, the second fault runs north-south, creating a steep topographic sequence, and the last fault has a northeast-southwest orientation, resulting in steep topography from west to east. A visual representation of the geological conditions is illustrated in Figure 2 (source: <https://geologi.esdm.go.id/>).

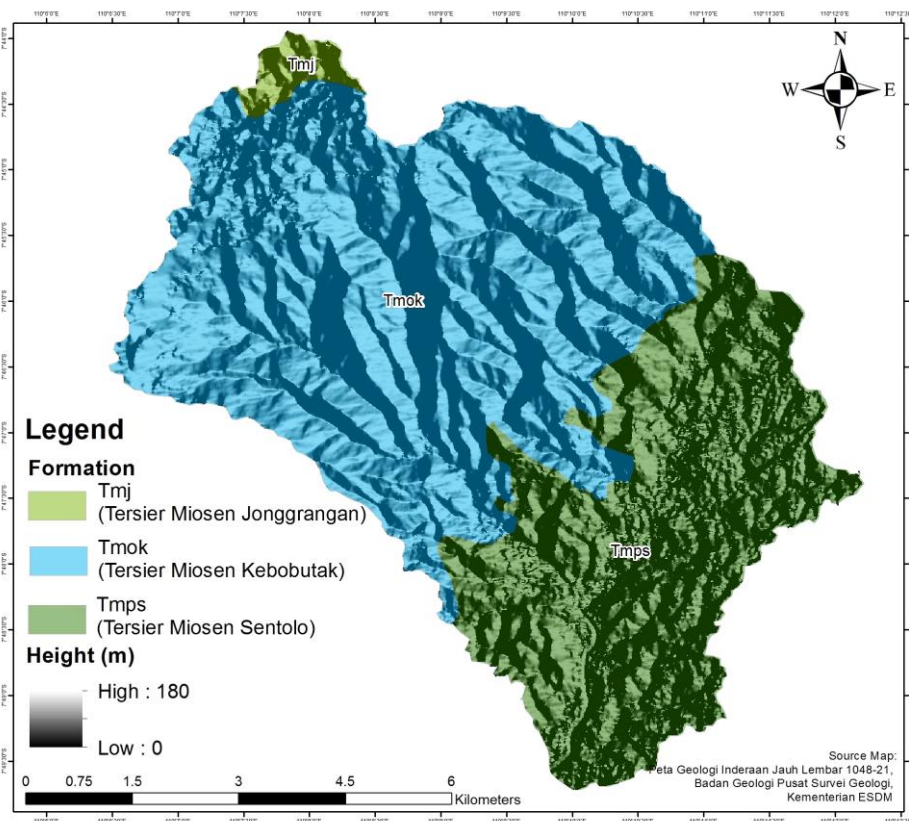


Figure 2. Geological condition of the research area

### 3. Data

Five parameters were used to generate landslide susceptibility zonation using combinations of TRIGRS and Flow-R. The first parameter, slope, derived from the Digital Elevation Model (DEM), is universally acknowledged as a critical factor in landslide susceptibility, as it directly influences the gravitational forces acting on a slope [40]. Soil properties (e.g., cohesion, internal friction angle, and unit weight), groundwater level, and soil thickness were obtained through field investigations and laboratory tests. These parameters are essential for assessing slope stability and are key inputs for TRIGRS, which calculates changes in shear strength and pore water pressure resulting from rainfall infiltration [33, 36]. The final parameter, rainfall intensity, is a primary landslide trigger in the study area. Rainfall intensity is a crucial input for TRIGRS, driving the simulation of transient infiltration and its effect on slope stability [36]. Rainfall values were adopted from a previous study proposed by Rifai et al. [4]. Landslide inventories in the research area are also needed to measure the performance of the susceptibility zonation [41]. Details of each parameter used are as follows:

#### 3.1. Digital Elevation Model (DEM)

The topographic information employed in this research used the National Digital Elevation Model (DEMNAS), which can be accessed at (<https://tanahair.indonesia.go.id/demnas/>). DEMNAS possesses a spatial resolution of 0.27 arcseconds, corresponding to 8.1 meters, and utilizes the EGM 2008 vertical datum. In this context, arcseconds represent a unit of distance in raster data, signifying the distance between adjacent pixel cells. The topographic data was derived using ArcGIS software, and this data supplied essential information on slope inclination within the study area. The study area's topography, illustrated in Figure 3, exhibits significant elevation variations ranging from 14 to 842 meters. The higher elevations are concentrated in the upper part of the study area, while the lower elevations are found in the bottom section. The DEM data plays a crucial role in constructing a surface flow direction model, facilitating the assessment of water distribution and runoff routing in the research area.

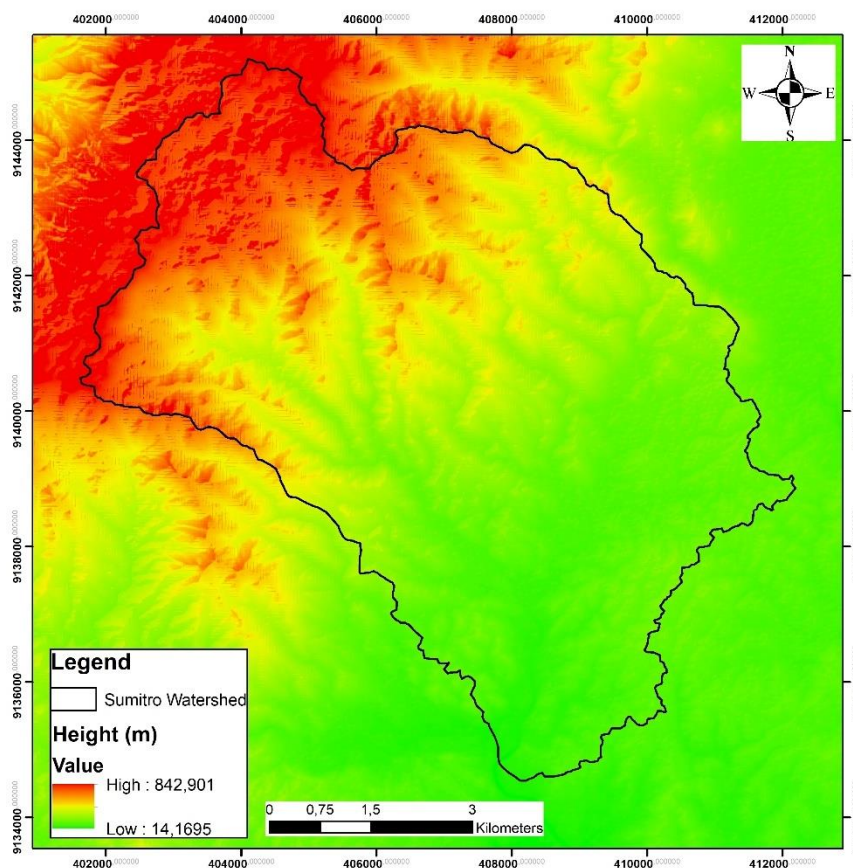


Figure 3. Digital Elevation Model of Sumitro Watershed

#### 3.2. Soil Properties, Groundwater Level, and Soil Thickness

The soil properties data were obtained through laboratory testing using nine soil samples collected directly from the research site (Figure 4-a shows the method used to get the soil sample). The soil properties data consist of hydraulic and mechanical values of the soil. The hydraulic properties are diffusivity, saturated permeability coefficient ( $k$ ), residual moisture content ( $\theta_r$ ), saturation moisture content ( $\theta_s$ ), and the inverse of capillary water height ( $\alpha$ ). The mechanical properties are bulk density ( $\gamma$ ), cohesion ( $c$ ), and internal friction angle ( $\phi$ ). All of the soil properties were obtained

from laboratory-scale testing. Besides the soil properties, an investigation of groundwater level and soil thickness was also conducted in the study area. Groundwater level measurement is based on the water level in wells or springs found at the research location (shown in Figure 4-b), while the soil thickness is based on the visual observation of the exposed soil layer (shown in Figure 4-c). In total, there were nine points of groundwater level measurement and ten points of soil thickness observation from the study area. The distribution of soil sampling, groundwater level measurements, and soil thickness observations is shown in Figure 5.



Figure 4. (a) Soil sampling (b) GWL measurement (c) soil thickness observation

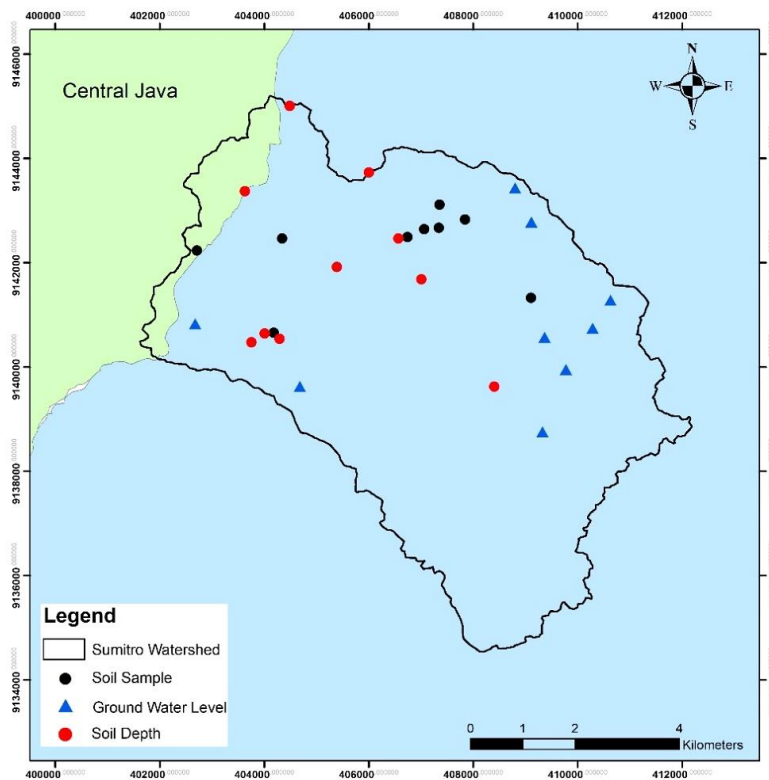


Figure 5. Distribution of soil sampling, GWL, and soil thickness observation

Simplification needs to be done on the geotechnical data that has been obtained to get good TRIGRS results [24, 42]. In this study, the mean value of soil properties, groundwater level measurement, and soil thickness observation were chosen to represent the study area [43]. Table 1 shows the resume of the soil properties, groundwater level measurement, and soil thickness observation used in this study.

Table 1. Soil investigation result of the study area (in average)

Soil hydraulic properties					Soil mechanical properties			GWL (m)	Soil Thickness (m)
dif (m/s)	k (m/s)	$\theta_s$	$\theta_r$	$\alpha$	c (N/m <sup>2</sup> )	$\phi$ (°)	$\gamma$ (N/m <sup>3</sup> )		
$2.4 \times 10^{-3}$	$1.23 \times 10^{-6}$	0.23	0.06	0.09	14.100	35	22.300	5.1	2.2

### 3.3. Rainfall Intensity

Rainfall intensity is a parameter that often triggers landslides; many landslide events occur during the rainy season [44]. Estimating rainfall intensity that can trigger landslides (rainfall threshold) always becomes an interesting topic for

discussion. Rainfall thresholds for landslides may differ based on each area's characteristics [45]. In order to identify the landslide potential of the research area, the rainfall threshold for landslide was used as an input to TRIGRS. The rainfall threshold used is based on research conducted in the near study area by Rifai et al. [4], with an intensity value of 44 mm/day. Rifai et al. [4] calculated rainfall thresholds using rainfall data from Singkung Rainfall Station from 2016 to 2021. The research took place in the Girimulyo district, under the Kulon Progo regency, part of Menorah Mountain. The single rainfall value was applied to the whole research area.

### 3.4. Landslide Inventories

Information on landslide events was obtained from the local government and communities; this data was verified through field investigation using the method proposed by Samodra et al. [46]. The landslide events recorded in this study are those with a minimum width of 5 m × 5 m. In total, 99 landslide events were selected as landslide inventories during 2012–2021. Most of the landslide events are located in the upper part of the research area, where the slope is relatively steeper than the other part. Examples of landslide events in the study area are shown in Figure 6, while the landslide inventories are shown in Figure 7.



Figure 6. Example of landslide events in the research area

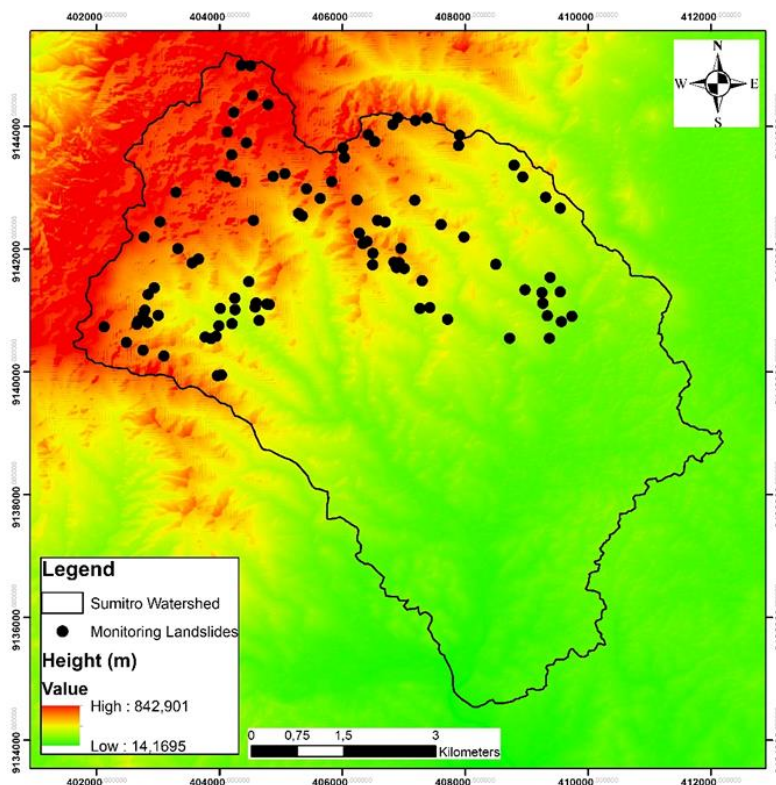


Figure 7. Landslide inventories in study area 2012-2021

## 4. Method

Five parameters—slope, soil properties, groundwater level, soil thickness, and rainfall—were used as inputs in TRIGRS to create the landslide initiation zonation. The TRIGRS result, along with the DEM, was then used as input in Flow-R to produce the final landslide susceptibility zonation. Meanwhile, the landslide inventory was obtained from local governments and communities, and field investigations were conducted to validate the data. The selected landslide inventory was then used to calculate the Area Under the Curve (AUC) for both TRIGRS and the TRIGRS-Flow-R combination. The overall workflow of this study is shown in Figure 8.

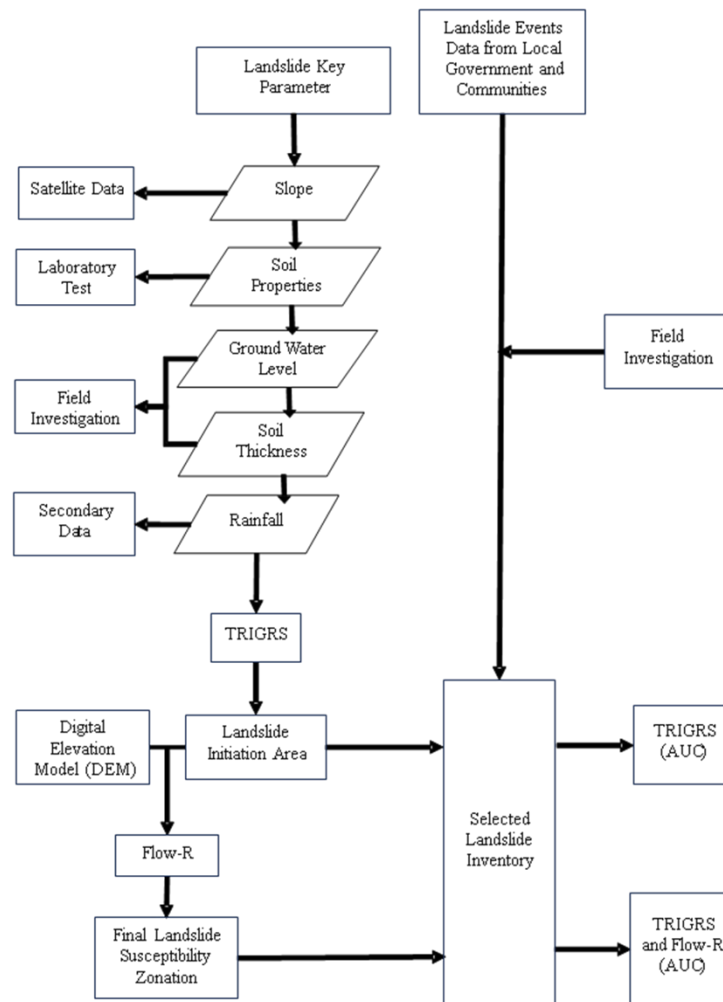


Figure 8. The workflow of this study

### 4.1. Identification of Source Area

Transient Rainfall Infiltration and Grid-based Regional Slope Stability (TRIGRS) is a computational program written in the FORTRAN language, designed to model the transient effects of rainfall infiltration on slope stability by calculating changes in groundwater column height and safety factors of slopes [36, 38]. This program integrates hydrological and geotechnical processes, providing a physically-based approach to assessing rainfall-induced landslides. TRIGRS calculates rainfall infiltration into the soil, simulating the increase in pore-water pressure and its impact on slope stability. The model assumes Darcy's law governs the infiltration process and applies a simplified version of Richard's equation to evaluate unsaturated and saturated flow conditions. The parameters computed are output in ".ascii" format, representing numerical values within grid cells. They can be easily linked to Geographic Information System (GIS) software for visualization and spatial analysis of results. The spatial resolution of TRIGRS outputs aligns with the input Digital Elevation Model (DEM) data, which, in this study, has a resolution of 0.27 arcseconds, equivalent to 8.1 meters. The parameters used in TRIGRS include rainfall, slope gradient, soil depth, groundwater level, soil permeability, soil diffusivity, volumetric and residual water content, cohesion, internal friction angle, and soil unit weight.

Theoretically, TRIGRS uses a 3D coordinate system (xyz) to model the interaction of rainfall infiltration and slope stability [33]. The slope-stability analysis is based on the limit equilibrium method, where the safety factor is determined as the ratio of resisting forces (shear strength of the soil) to driving forces (shear stress induced by gravity and pore

water pressure). Rainfall infiltration increases the pore-water pressure, reducing the soil's effective stress and decreasing its shear strength [37]. The TRIGRS model employs a linearized solution of Richards' equation for unsaturated flow, coupled with analytical equations for saturated flow, to calculate transient pore-pressure changes [47]. These calculations are based on de Luiz Rosito Listo et al. [33] and Guzzett et al. [44] works, which provide a detailed derivation of the hydrological model and its application to slope stability. Specifically, TRIGRS considers the geometry of the slope by utilizing the xyz coordinate system, where x represents slope inclination, y represents topographic contours, and z represents vertical depth relative to the x-y plane. The horizontal slope angle is denoted by  $\delta$ . The vertical depth ( $Z$ ) within this framework is described by Equation 1:

$$Z = x \sin \delta + z \cos \delta \quad (1)$$

If the depths  $Z$  and  $z$  are equal, the equation simplifies to  $Z = z/\cos \delta$ .

This theoretical approach allows TRIGRS to predict landslide initiation due to rainfall infiltration [36]. By combining hydrological and geotechnical theories, TRIGRS provides detailed and spatially explicit predictions of slope stability. This capability is valuable for determining landslide susceptibility zonation, as it identifies areas prone to slope failure with high accuracy.

## 4.2. Run-Out Modeling

The source area obtained from TRIGRS and topography data was used as the main input to create a susceptibility map with Flow-R. Flow-R is a flow assessment of gravitational hazard on a regional scale [48]. Flow-R was first introduced by Pascal et al. [49]. This program uses Matlab to calculate the spreading area of debris flow [49]. Flow-R has been used to estimate debris flow susceptibility maps in several places, showing promising results [11, 48]. Flow-R only shows results in the probabilistic area that may be affected by the landslide, and it does not give information about the volume or velocity of the landslide [48].

The propagation of run-out modeling in flow-R is divided into two steps: calculate the direction in which debris flow will follow and the run-out distance [49]. The flow direction calculation is based on research by Horton et al. [39]. The run-out distance calculation using simple energy balance algorithms is shown in Equation 2 [49].

$$E_{kin}^i = E_{kin}^0 + \Delta E_{pot}^i - E_f^i \quad (2)$$

where  $E^i_{kin}$  is the kinetic energy of the cell in direction  $i$ ,  $E^0_{kin}$  is the kinetic energy of the central cell,  $E^i_{pot}$  is the change in potential energy to the cell in direction  $i$ , and  $E^i_f$  is the energy lost in friction to the cell in direction  $i$ . Some conditions are defined so that there is always at least one cell where the flow can run so that run-out distance algorithms only determine if it flows further or stops [49]. Data needed to run the Flow-R beside the source area is only DEM.

## 4.3. Validation

Statistical validation using Area Under Curve (AUC) based on landslide and debris flow inventories was applied to derive the model performance. AUC is generated from the Receiver Operating Characteristic (ROC) curve based on sensitivity and specificity value [17, 50]. To calculate the AUC, the sensitivity (True Positive Rate) and 1-specificity (1-True Negative Rate) were plotted against each other in the graph across various thresholds [51]. This study calculated sensitivity and specificity by comparing the landslide susceptibility map generated from the model with the observed landslide inventory. The susceptibility map was reclassified into two categories: stable and unstable. Unstable areas represent high landslide susceptibility zones, while stable areas represent low susceptibility zones. Sensitivity measures the proportion of correctly identified unstable areas relative to all actual unstable areas, as determined by the landslide inventory, while specificity measures the proportion of correctly identified stable areas relative to all actual stable areas, as derived from regions not included in the landslide inventory. A higher sensitivity indicates that the model effectively captures most of the observed landslide events, while higher specificity suggests that the model accurately excludes stable areas from being falsely classified as unstable.

AUC values range from 0 to 1, where a value of 1.0 represents perfect accuracy, 0.5 indicates no predictive power (equivalent to random guessing), and values below 0.5 suggest poor performance [5]. The minimum value of AUC to show good performance is higher than 0.6 or categorized as satisfactory [15], as it demonstrates the model's ability to capture the underlying relationship between input parameters and observed landslides. Further, Yang & Berdine [52] categorized an AUC value of 0.6-0.7 as an acceptable correlation where the model provides fair predictive capability, 0.7-0.8 as an excellent correlation showing strong predictive power and reliable identification of landslide-prone areas, and above 0.8 as an outstanding correlation where the model is highly accurate in its predictions.

## 5. Results and Discussion

### 5.1. Landslide Susceptibility Zonation Based on TRIGRS

The TRIGRS model was used to calculate the Safety Factor (SF) based on five parameter inputs, as described before. The results of the TRIGRS modeling are shown in (Figure 9). The result is divided into two classes based on stability, which represents the SF value. Following the existing regulation (SNI) No.8291 on Determination and Compilation of Landslide Zonation [53], the area is considered as high movement (unstable) if the SF is less than 1.2 and vice versa. The unstable area is displayed in red and magenta color, while the stable area is in yellow and green color.

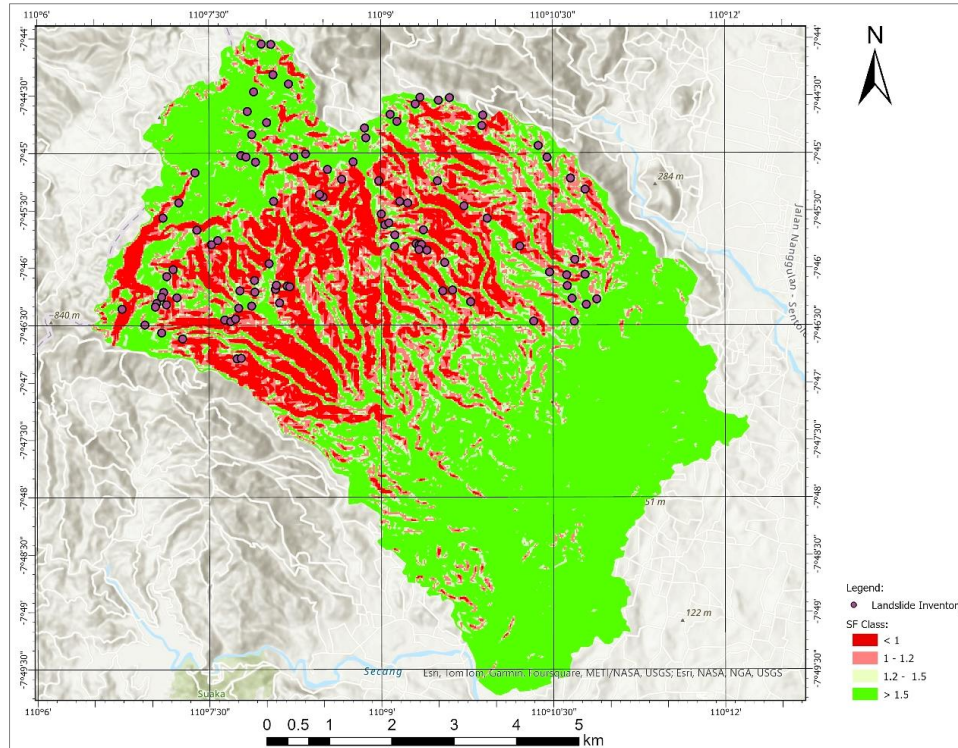


Figure 9. TRIGRS Susceptibility Landslide Zonation

Results of the TRIGRS show that most study areas belong to the stable class with a wide area of around 4770 ha (69%), while the unstable area is around 1042 Ha (31%). Most of the unstable areas are located in the middle of the map. (Figure 9) also shows the landslide location collected in this study. In total, more than half of the landslide events were located in the unstable zone, precisely 68%. This result leads to an AUC value of 0.679 for landslide susceptibility zonation, as shown in Figure 10. The AUC value of 0.679 shows an acceptable relationship between landslide susceptibility zonation generated by TRIGRS and landslide inventories [52].

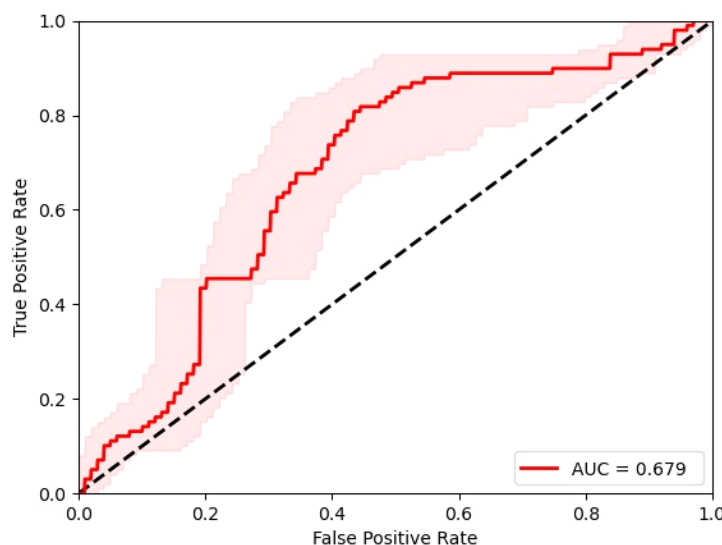


Figure 10. AUC for TRIGRS Susceptibility Landslide Zonation

Based on Figure 2, the geological setting of the study area is divided into two major formations. The Kebobutak Formation dominates the upper to middle portions of the map, while the Sentolo Formation occupies the lower sections. Most landslides in the study area occur within the Kebobutak Formation, making it the most vulnerable zone to slope failures. This heightened susceptibility is due to a combination of geological, topographical, and hydrological factors. The Kebobutak Formation is composed of sandstone, silt, clay, tuff, and agglomerate, which are inherently weaker compared to the marl, limestone, and agglomerate that constitute the Sentolo Formation. Clay and silt layers tend to retain water, leading to increased pore water pressure during rainfall, while tuff and agglomerate weather easily, breaking down into weaker materials over time. The high permeability of sandstone and tuff facilitates significant rainfall infiltration, often creating perched water tables that destabilize slopes. In contrast, the Sentolo Formation is less susceptible to landslides. Its materials, particularly limestone and marl, are more durable and resistant to weathering. Additionally, the low permeability of limestone and marl reduces pore pressure buildup, contributing to greater slope stability. The topographical differences also play a key role in slope stability. The Kebobutak Formation is characterized by relatively steep slopes and higher topographic values compared to the Sentolo Formation. These steeper slopes amplify gravitational forces, further reducing the stability of the terrain. Together, these factors explain why most landslides occur within the Kebobutak Formation.

## 5.2. Landslide Susceptibility Zonation with a Combination of TRIGRS and Flow-R

Based on the identification of the landslide source area with TRIGRS combined with DEM data, Flow-R is then run to model the run-out. Only the very high and high classes are used as landslide source areas in Flow-R; this is because those classes have SF below 1.2, which is categorized as an unstable slope. The result of the TRIGRS-Flow-R susceptibility modeling is shown in Figure 11. The susceptibility zonation map was divided into four classes, namely: very high (red), high (magenta), moderate (yellow), and low (green).

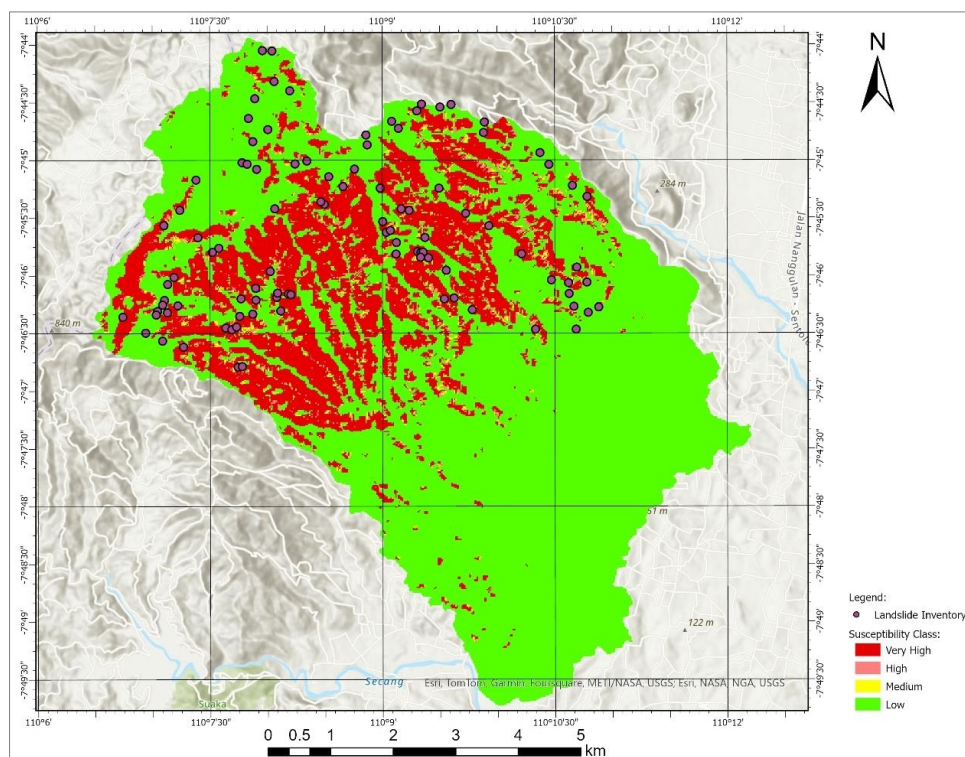


Figure 11. TRIGRS-Flow-R Debris Flow Susceptibility Zonation

Figure 11 shows a wider unstable area compared to (Figure 9) because of the run-out modeling with flow-R. In summary, the unstable area increased from 1042 ha to 1506 ha, while the stable area decreased accordingly. The addition of 464 hectares of unstable area is attributed to the possibility that a landslide could trigger a debris flow, as modeled by Flow-R. The direction of landslide material follows the contour, flowing toward areas with lower slopes. The study area is located in a mountainous region characterized by high topography and steep slopes, which significantly influence the run-out behavior of landslide material. Steeper slopes provide greater gravitational force, allowing the landslide materials to travel faster and farther. High topographic relief further amplifies the potential energy available to debris, resulting in extended run-out distances. As the material descends, it often follows natural channels or gullies, spreading further when it reaches flatter terrain.

The AUC value for this combined landslide susceptibility map increased from 0.679 to 0.728, as shown in Figure 12. This result also indicated that the combined landslide susceptibility map correlates better with the landslide inventories. Based on Yang & Berdine [52], an AUC value of 0.728 indicates an “excellent” correlation between the landslide susceptibility map and landslide events, while an AUC value of 0.679 only gives an “acceptable” correlation. The additional unstable area in the susceptibility zonation is the primary factor contributing to increasing the AUC value. The integration of run-out modeling makes the landslide's impact wider, which is not considered in standard landslide susceptibility zonation. In run-out modeling, besides topography and slope, other parameters contributing to the susceptibility zonation expansion include soil characteristics such as friction angle and flow mobility. These parameters are critical in determining how far and in which direction the landslide material travels. A lower friction angle indicates weaker resistance to movement, allowing debris to travel further downslope, while high flow mobility enables the material to spread out over a wider area, particularly in flatter terrains or channels. When combined with steep slopes and high topography, these factors significantly influence the accuracy of run-out predictions and, consequently, the overall susceptibility zonation. This integration ensures that areas previously considered stable in standard susceptibility zonation are now recognized as potentially unstable due to their proximity to potential run-out paths. This holistic approach improves the model's predictive performance, as reflected in the increased AUC value, and enhances its applicability for disaster risk management and mitigation planning, particularly in mountainous regions with complex topography.

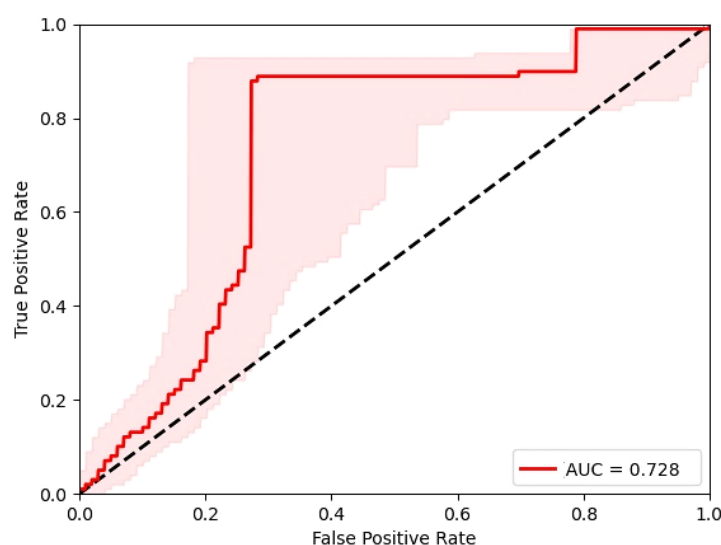


Figure 12. AUC for TRIGRS-Flow-R Debris Flow Susceptibility Zonation

### 5.3. Discussion

Landslide susceptibility zonation is one of the simplest ways to identify areas prone to landslide hazards. Several methods can be used to create landslide susceptibility zonation. According to Do et al. [11] at least three methods are commonly employed: Heuristic, Statistical, and Deterministic. Among these, the heuristic approach is the most generalized, suitable for covering broader areas but with less detail. In contrast, while requiring more extensive data, the deterministic method provides the most detailed results, making it the most effective approach for generating landslide susceptibility zonation in smaller areas where precise data can be obtained. TRIGRS is a deterministic method that calculates the Safety Factor (SF) to determine susceptibility zones. Several researchers have explored combining Flow-R with various landslide initiation models, yielding promising results. Do et al. [11] compared landslide susceptibility zonation generated using a combination of Analytical Hierarchy Process (AHP), Weights of Evidence (WoE), and Logistic Regression (LR) with Flow-R. In this approach, AHP, WoE, and LR were used to identify landslide initiation, while Flow-R was used to propagate the run-out.

Similarly, Rahman et al. [16] combined AHP with Flow-R to create a landslide susceptibility zonation. However, the combination of TRIGRS and Flow-R to generate landslide susceptibility zonation has not been done before. This study explores this novel approach, integrating TRIGRS to identify landslide initiation zones and Flow-R to model the run-out, providing new insights into creating more accurate and detailed landslide susceptibility zonation. (Figure 13) summarizes studies that have attempted to combine AHP, WoE, LR, and TRIGRS with Flow-R to create landslide susceptibility zonation.

Based on Figure 13, the best AUC result comes from the combination of AHP-Flow-R by Rahman et al. [16], with an AUC value of 0.980. Following this are the combinations of WoE-Flow-R and LR-Flow-R, which achieved AUC values of 0.882 and 0.865, respectively. Next is the combination of AHP-Flow-R by Do et al. [11], with an AUC value

of 0.829. Notably, although both studies used the same AHP method, their AUC results differ. This condition is likely due to different conditions of the research area, the quality of the landslide inventory data, or the various parameters used to establish the landslide susceptibility zonation. In summary, all four studies above show very good AUC results, with values above 0.8, indicating an outstanding correlation between the landslide susceptibility zonation and the landslide inventory [38].

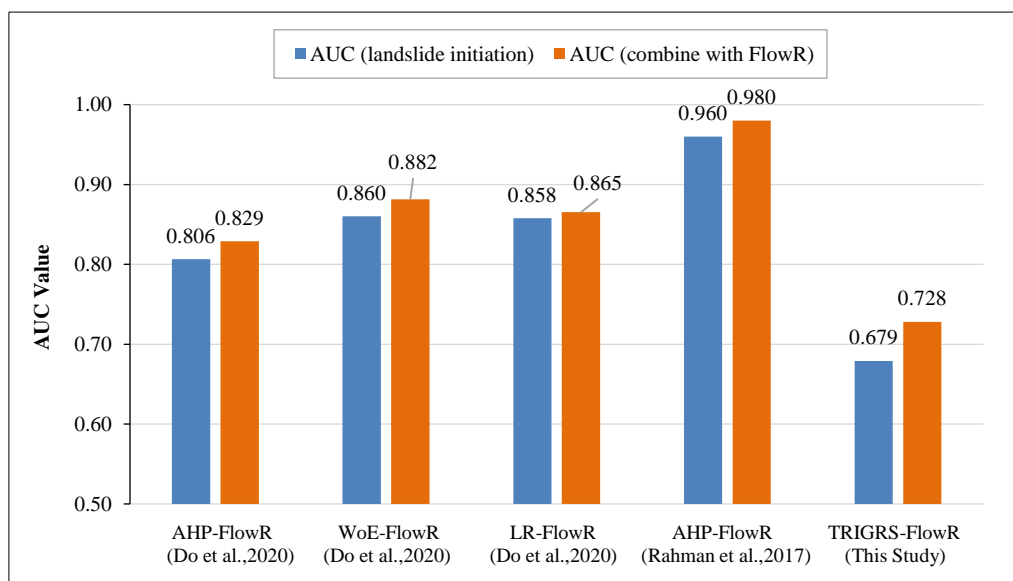


**Figure 13. Previous study in combination of AHP, WoE and LR with Flow-R**

The TRIGRS method used in this study showed an AUC value of 0.679, which is considered an “acceptable” correlation between the model results and the landslide inventory [52]. However, TRIGRS had the lowest AUC compared to other methods used for landslide initiation. This result was unexpected, as deterministic methods like TRIGRS typically yield higher AUC values than heuristic methods like AHP, WoE, and LR. The data quality used in the deterministic model likely impacted the results. The process of collecting field data was less than ideal due to the challenging terrain in the research area. Due to challenging field conditions, soil sampling, groundwater level observations, and soil thickness measurements could only be conducted at a limited number of points. The tropical climate in the research area led to dense vegetation cover, making accurate soil thickness measurements difficult. Soil sampling was performed using simple manual tools, such as tubes inserted into the ground, as illustrated in (Figure 4.a). This method restricted sampling to shallow depths of less than one meter and limited the locations where samples could be collected.

Similarly, groundwater level measurements were only possible at sites with existing wells or springs, further limiting the spatial coverage of the data. The uneven distribution of sampling locations, combined with the small number of data points, resulted in an incomplete representation of the study area (Figure 5). To address this problem, we averaged the data collected from the field and used it as a single representative value for the entire area. This approach, however, may have contributed to the unexpected performance of TRIGRS, as the use of averaged data likely reduced the accuracy of the model's predictions.

Despite these limitations, the integration of TRIGRS with Flow-R in this study improved the overall model performance. The combined TRIGRS-Flow-R model produced an AUC value of 0.728, which is a significant increase compared to using TRIGRS alone, with an AUC value of 0.679. The nearly 0.05 increase in AUC was a very significant improvement compared to other studies listed above. Other studies demonstrated only small increases in AUC values. The smallest improvement was seen in the LR-Flow-R combination, with an increase of just 0.007. Followed by the combination of AHP-Flow-R by Rahman et al. [16] with a 0.02 increase. The combinations of WoE-Flow-R and AHP-Flow-R by Do et al. [11] showed slightly higher increases, at 0.022 and 0.023, respectively. These findings suggest that, among the various methods tested, the TRIGRS-Flow-R combination is particularly effective, offering promising results that could be replicated in other regions. This improvement highlights the potential of combining deterministic models like TRIGRS, which excel in identifying initiation zones, with Flow-R, a tool that is effective for modeling the run-outs.

Another issue in establishing landslide susceptibility zonation is that many stable areas are incorrectly classified as unstable (False Positive Rate / FPR), leading to an overestimation of landslide susceptibility zonation. This condition can raise another problem, such as eroding trust in the model's predictions, increased costs for infrastructure

development in areas that are not hazardous, and even reducing the overall efficiency of risk mitigation strategies. In order to overcome this problem, field verification and community-based approaches can be applied. Field verification involves conducting on-site assessments to validate areas categorized as unstable by the model. This process provides ground-truth data, helping to identify and correct inaccuracies in the susceptibility zonation and improving its reliability by incorporating real observations. Additionally, community-based approaches leverage local knowledge about historical landslides, terrain conditions, and other contextual factors that the model might not capture. Engaging local communities in the verification process of landslide susceptibility assessment improves the accuracy of the landslide susceptibility zonation and fosters trust and collaboration between stakeholders. By combining field verification with community input, false positives can be reduced, ensuring that the landslide susceptibility zonation is accurate and practical for application.

## 6. Conclusion

This study addresses the critical need for improved landslide susceptibility zonation, particularly in mountainous regions characterized by steep slopes and high rainfall intensity. Standard landslide susceptibility models often focus solely on identifying landslide-prone areas without considering secondary hazards, such as the propagation of landslide material, which can exacerbate the impact. In order to address this limitation, this research integrates hydrological and geotechnical modeling (TRIGRS) with run-out analysis (Flow-R) to provide a more comprehensive assessment. The results demonstrate that TRIGRS effectively identifies landslide-prone areas, achieving an AUC value of 0.679, which is considered acceptable. However, landslides often extend beyond their initiation points due to material propagation triggered by rainfall. By incorporating Flow-R to simulate run-out modeling, the AUC value increased to 0.728, indicating enhanced accuracy and a better correlation between the susceptibility map and landslide inventories. This improvement underscores the importance of including run-out modeling to capture the full extent of potential landslide impacts.

While the integration of run-out analysis improves model accuracy, it also increases the size of the unstable zone, which leads to a higher False Positive Rate (overestimating the landslide susceptibility zone). In the case of disaster mitigation efforts, taking preventive steps against the risk of disaster threats would be better. In this case, making a landslide susceptibility zonation map with the addition of landslide material propagation is a wise choice. To minimize the False Positive Rate, field-based validation and community-based participatory mapping are recommended. These strategies not only improve the accuracy of susceptibility zonation maps but also enhance their practical usability, supporting local disaster preparedness initiatives. In conclusion, a combined approach of TRIGRS and Flow-R sets a benchmark for future studies and provides valuable insights into improving landslide susceptibility zonation, particularly in regions prone to cascading hazards.

## 7. Declarations

### 7.1. Author Contributions

Conceptualization, A.R. and R.A.; methodology, R.A. and F.F.; software, T.R., B.R., E.P., and B.W.; validation, E.P. and B.W.; formal analysis, R.A., E.P., and B.W.; investigation, A.R. and R.A.; resources, R.A.; data curation, T.R. and B.R.; writing—original draft preparation, A.R. and R.A.; writing—review and editing, A.R., F.F., and R.A.; visualization, R.A., E.P., and B.W.; supervision, A.R. and F.F.; project administration, A.R.; funding acquisition, A.R. All authors have read and agreed to the published version of the manuscript.

### 7.2. Data Availability Statement

The data presented in this study are available on request from the corresponding author.

### 7.3. Funding

This research supported by Kementerian Pendidikan, Kebudayaan, Riset dan Teknologi under research grant No: 0277/E5/AK.04/2022.

### 7.4. Acknowledgements

The authors would thank Balai Teknik Sabo for supporting the Flow-R program. The authors also thank Riza, Lukman, Nabilla, Agus, and Dwi from the Civil and Environmental Department UGM for supporting this research.

### 7.5. Conflicts of Interest

The authors declare no conflict of interest.

## 8. References

- [1] Park, D. W., Nikhil, N. V., & Lee, S. R. (2013). Landslide and debris flow susceptibility zonation using TRIGRS for the 2011 Seoul landslide event. *Natural Hazards and Earth System Sciences*, 13(11), 2833–2849. doi:10.5194/nhess-13-2833-2013.
- [2] Pecoraro, G., Calvello, M., & Piciullo, L. (2019). Monitoring strategies for local landslide early warning systems. *Landslides*, 16(2), 213–231. doi:10.1007/s10346-018-1068-z.
- [3] Piciullo, L., Calvello, M., & Cepeda, J. M. (2018). Territorial early warning systems for rainfall-induced landslides. *Earth-Science Reviews*, 179, 228–247. doi:10.1016/j.earscirev.2018.02.013.
- [4] Rifai, A., Andika Yuniawan, R., Faris, F., Subiyantoro, A., Sidik, V., & Prayoga, H. (2022). Performance of rainfall satellite threshold to predict landslide events in Girimulyo District. 2022 IEEE International Conference on Aerospace Electronics and Remote Sensing Technology (ICARES), 1–6. doi:10.1109/icares56907.2022.9993592.
- [5] Yuniawan, R. A., Rifa'i, A., Faris, F., Subiyantoro, A., Satyaningsih, R., Hidayah, A. N., Hidayat, R., Mushthofa, A., Ridwan, B. W., Priangga, E., Muntohar, A. S., Jetten, V. G., Westen, C. J. van, Bout, B. V. den, & Sutanto, S. J. (2022). Revised Rainfall Threshold in the Indonesian Landslide Early Warning System. *Geosciences*, 12(3), 129. doi:10.3390/geosciences12030129.
- [6] Hadmoko, D. S., Lavigne, F., Sartohadi, J., Hadi, P., & Winaryo. (2010). Landslide hazard and risk assessment and their application in risk management and landuse planning in eastern flank of Menoreh Mountains, Yogyakarta Province, Indonesia. *Natural Hazards*, 54(3), 623–642. doi:10.1007/s11069-009-9490-0.
- [7] Abbaszadeh Shahri, A., Spross, J., Johansson, F., & Larsson, S. (2019). Landslide susceptibility hazard map in southwest Sweden using artificial neural network. *Catena*, 183, 104225. doi:10.1016/j.catena.2019.104225.
- [8] Broeckx, J., Vanmaercke, M., Duchateau, R., & Poesen, J. (2018). A data-based landslide susceptibility map of Africa. *Earth-Science Reviews*, 185, 102–121. doi:10.1016/j.earscirev.2018.05.002.
- [9] Bălăceanu, D., Micu, M., Jurchescu, M., Malet, J. P., Sima, M., Kucsicsa, G., Dumitrică, C., Petrea, D., Mărgărint, M. C., Bilașco, Ș., Dobrescu, C. F., Călărașu, E. A., Olinic, E., Boți, I., & Senzaconi, F. (2020). National-scale landslide susceptibility map of Romania in a European methodological framework. *Geomorphology*, 371, 107432. doi:10.1016/j.geomorph.2020.107432.
- [10] Polykretis, C., Ferentinou, M., & Chalkias, C. (2014). A comparative study of landslide susceptibility mapping using landslide susceptibility index and artificial neural networks in the Krios River and Krathis River catchments (northern Peloponnese, Greece). *Bulletin of Engineering Geology and the Environment*, 74(1), 27–45. doi:10.1007/s10064-014-0607-7.
- [11] Do, H. M., Yin, K. L., & Guo, Z. Z. (2020). A comparative study on the integrative ability of the analytical hierarchy process, weights of evidence and logistic regression methods with the Flow-R model for landslide susceptibility assessment. *Geomatics, Natural Hazards and Risk*, 11(1), 2449–2485. doi:10.1080/19475705.2020.1846086.
- [12] Stanley, T., & Kirschbaum, D. B. (2017). A heuristic approach to global landslide susceptibility mapping. *Natural Hazards*, 87(1), 145–164. doi:10.1007/s11069-017-2757-y.
- [13] Hasekiogulları, G. D., & Ercanoğlu, M. (2012). A new approach to use AHP in landslide susceptibility mapping: A case study at Yenice (Karabuk, NW Turkey). *Natural Hazards*, 63(2), 1157–1179. doi:10.1007/s11069-012-0218-1.
- [14] Pourghasemi, H. R., Pradhan, B., & Gokceoglu, C. (2012). Application of fuzzy logic and analytical hierarchy process (AHP) to landslide susceptibility mapping at Haraz watershed, Iran. *Natural Hazards*, 63(2), 965–996. doi:10.1007/s11069-012-0217-2.
- [15] Sonker, I., Tripathi, J. N., & Singh, A. K. (2021). Landslide susceptibility zonation using geospatial technique and analytical hierarchy process in Sikkim Himalaya. *Quaternary Science Advances*, 4, 100039. doi:10.1016/j.qsa.2021.100039.
- [16] Rahman, M. S., Ahmed, B., & Di, L. (2017). Landslide initiation and runoff susceptibility modeling in the context of hill cutting and rapid urbanization: a combined approach of weights of evidence and spatial multi-criteria. *Journal of Mountain Science*, 14(10), 1919–1937. doi:10.1007/s11629-016-4220-z.
- [17] Goyes-Peñafiel, P., & Hernandez-Rojas, A. (2021). Landslide susceptibility index based on the integration of logistic regression and weights of evidence: A case study in Popayan, Colombia. *Engineering Geology*, 280, 105958. doi:10.1016/j.enggeo.2020.105958.
- [18] Conforti, M., & Ietto, F. (2021). Modeling shallow landslide susceptibility and assessment of the relative importance of predisposing factors, through a GIS-based statistical analysis. *Geosciences (Switzerland)*, 11(8), 333. doi:10.3390/geosciences11080333.
- [19] Huang, S., & Chen, L. (2024). Landslide susceptibility mapping using an integration of different statistical models for the 2015 Nepal earthquake in Tibet. *Geomatics, Natural Hazards and Risk*, 15(1), 2396908. doi:10.1080/19475705.2024.2396908.
- [20] Wang, Y., Wang, L., Liu, S., Liu, P., Zhu, Z., & Zhang, W. (2023). A comparative study of regional landslide susceptibility mapping with multiple machine learning models. *Geological Journal*, 59(9), 2383–2400. doi:10.1002/gj.4902.

- [21] Aditian, A., Kubota, T., & Shinohara, Y. (2018). Comparison of GIS-based landslide susceptibility models using frequency ratio, logistic regression, and artificial neural network in a tertiary region of Ambon, Indonesia. *Geomorphology*, 318, 101–111. doi:10.1016/j.geomorph.2018.06.006.
- [22] Choi, J., Oh, H. J., Lee, H. J., Lee, C., & Lee, S. (2012). Combining landslide susceptibility maps obtained from frequency ratio, logistic regression, and artificial neural network models using ASTER images and GIS. *Engineering Geology*, 124(1), 12–23. doi:10.1016/j.enggeo.2011.09.011.
- [23] Tang, R. X., Kulatilake, P. H. S. W., Yan, E. C., & Cai, J. Sen. (2020). Evaluating landslide susceptibility based on cluster analysis, probabilistic methods, and artificial neural networks. *Bulletin of Engineering Geology and the Environment*, 79(5), 2235–2254. doi:10.1007/s10064-019-01684-y.
- [24] Marin, R. J., Velásquez, M. F., & Sánchez, O. (2021). Applicability and performance of deterministic and probabilistic physically based landslide modeling in a data-scarce environment of the Colombian Andes. *Journal of South American Earth Sciences*, 108, 103175. doi:10.1016/j.jsames.2021.103175.
- [25] Blais-Stevens, A., & Behnia, P. (2016). Debris flow susceptibility mapping using a qualitative heuristic method and Flow-R along the Yukon Alaska Highway Corridor, Canada. *Natural Hazards and Earth System Sciences*, 16(2), 449–462. doi:10.5194/nhess-16-449-2016.
- [26] Reichenbach, P., Rossi, M., Malamud, B. D., Mihir, M., & Guzzetti, F. (2018). A review of statistically-based landslide susceptibility models. *Earth-Science Reviews*, 180, 60–91. doi:10.1016/j.earscirev.2018.03.001.
- [27] Hong, H., Wang, D., Zhu, A. X., & Wang, Y. (2024). Landslide susceptibility mapping based on the reliability of landslide and non-landslide sample. *Expert Systems with Applications*, 243, 122933. doi:10.1016/j.eswa.2023.122933.
- [28] Agboola, G., Beni, L. H., Elbayoumi, T., & Thompson, G. (2024). Optimizing landslide susceptibility mapping using machine learning and geospatial techniques. *Ecological Informatics*, 81, 102583. doi:10.1016/j.ecoinf.2024.102583.
- [29] Lee, S., Jang, J., Kim, Y., Cho, N., & Lee, M. J. (2020). Susceptibility analysis of the Mt. Umyeon landslide area using a physical slope model and probabilistic method. *Remote Sensing*, 12(16), 2663. doi:10.3390/RS12162663.
- [30] Youssef, A. M., El-Haddad, B. A., Skilodimou, H. D., Bathrellos, G. D., Golkar, F., & Pourghasemi, H. R. (2024). Landslide susceptibility, ensemble machine learning, and accuracy methods in the southern Sinai Peninsula, Egypt: Assessment and Mapping. *Natural Hazards*, 120(15), 14227–14258. doi:10.1007/s11069-024-06769-w.
- [31] Doski, J. A. H. (2024). Landslide susceptibility evaluation in the mountainous terrain of the Zagros fold-thrust belt: a case study from Kurdistan, Northern Iraq. *Natural Hazards*. doi:10.1007/s11069-024-07069-z.
- [32] Berenguer, M., Sempere-Torres, D., & Hürlimann, M. (2015). Debris-flow forecasting at regional scale by combining susceptibility mapping and radar rainfall. *Natural Hazards and Earth System Sciences*, 15(3), 587–602. doi:10.5194/nhess-15-587-2015.
- [33] de Luiz Rosito Listo, F., Villaça Gomes, M. C., & Ferreira, F. S. (2021). Evaluation of shallow landslide susceptibility and Factor of Safety variation using the TRIGRS model, Serra do Mar Mountain Range, Brazil. *Journal of South American Earth Sciences*, 107, 103011. doi:10.1016/j.jsames.2020.103011.
- [34] Baum, R. L., & Godt, J. W. (2010). Early warning of rainfall-induced shallow landslides and debris flows in the USA. *Landslides*, 7(3), 259–272. doi:10.1007/s10346-009-0177-0.
- [35] Van Den Bout, B., Tang, C., Van Westen, C., & Jetten, V. (2022). Physically based modeling of co-seismic landslide, debris flow, and flood cascade. *Natural Hazards and Earth System Sciences*, 22(10), 3183–3209. doi:10.5194/nhess-22-3183-2022.
- [36] Baum, R. L., Savage, W. Z., & Godt, J. W. (2008). TRIGRS - A Fortran Program for Transient Rainfall Infiltration and Grid-Based Regional Slope-Stability Analysis, Version 2.0. Open-File Report. U.S. Geological Survey, Reston, United States. doi:10.3133/ofr20081159.
- [37] Muntohar, A. S., Prasetyaningtiyas, G. A., & Hidayat, R. (2021). The Spatial Model using TRIGRS to determine Rainfall-Induced Landslides in Banjarnegara, Central Java, Indonesia. *Journal of the Civil Engineering Forum*, 7(3), 289. doi:10.22146/jcef.55282.
- [38] Alvioli, M., & Baum, R. L. (2016). Parallelization of the TRIGRS model for rainfall-induced landslides using the message passing interface. *Environmental Modelling & Software*, 81, 122–135. doi:10.1016/j.envsoft.2016.04.002.
- [39] Horton, P., Jaboyedoff, M., Rudaz, B., & Zimmermann, M. (2013). Flow-R, a model for susceptibility mapping of debris flows and other gravitational hazards at a regional scale. *Natural Hazards and Earth System Sciences*, 13(4), 869–885. doi:10.5194/nhess-13-869-2013.
- [40] Susilo, A., Zulaikah, S., Pohan, A. F., Hasan, M. F. R., Hisyam, F., Rohmah, S., & Adhi, M. A. (2024). Vulnerability Index Assessment for Mapping Ground Movements Using the Microtremor Method as Geological Hazard Mitigation. *Civil Engineering Journal*, 10(5), 1616–1626. doi:10.28991/CEJ-2024-010-05-017.

- [41] Benmakhlouf, M., El Kharim, Y., Galindo-Zaldivar, J., & Sahrane, R. (2023). Landslide Susceptibility Assessment in Western External Rif Chain using Machine Learning Methods. *Civil Engineering Journal (Iran)*, 9(12), 3218–3232. doi:10.28991/CEJ-2023-09-12-018.
- [42] He, J., Qiu, H., Qu, F., Hu, S., Yang, D., Shen, Y., Zhang, Y., Sun, H., & Cao, M. (2021). Prediction of spatiotemporal stability and rainfall threshold of shallow landslides using the TRIGRS and Scoops3D models. *Catena*, 197, 104999. doi:10.1016/j.catena.2020.104999.
- [43] Marin, R. J., & Velásquez, M. F. (2020). Influence of hydraulic properties on physically modelling slope stability and the definition of rainfall thresholds for shallow landslides. *Geomorphology*, 351, 106976. doi:10.1016/j.geomorph.2019.106976.
- [44] Guzzetti, F., Peruccacci, S., Rossi, M., & Stark, C. P. (2007). Rainfall thresholds for the initiation of landslides in central and southern Europe. *Meteorology and Atmospheric Physics*, 98(3–4), 239–267. doi:10.1007/s00703-007-0262-7.
- [45] Segoni, S., Piciullo, L., & Gariano, S. L. (2018). A review of the recent literature on rainfall thresholds for landslide occurrence. *Landslides*, 15(8), 1483–1501. doi:10.1007/s10346-018-0966-4.
- [46] Samodra, G., Chen, G., Sartohadi, J., & Kasama, K. (2018). Generating landslide inventory by participatory mapping: an example in Purwosari Area, Yogyakarta, Java. *Geomorphology*, 306, 306–313. doi:10.1016/j.geomorph.2015.07.035.
- [47] Iverson, R. M. (2000). Landslide triggering by rain infiltration. *Water Resources Research*, 36(7), 1897–1910. doi:10.1029/2000WR900090.
- [48] Pastorello, R., Michelini, T., & D'Agostino, V. (2017). On the criteria to create a susceptibility map to debris flow at a regional scale using Flow-R. *Journal of Mountain Science*, 14(4), 621–635. doi:10.1007/s11629-016-4077-1.
- [49] Pascal, H., Michel, J., & Eric, B. (2008). Debris flow susceptibility mapping at a regional scale. *Proceedings of the 4<sup>th</sup> Canadian Conference on Geohazards: From Causes to Management*. Presse de l'Université Laval, Quebec, Canada.
- [50] Ávila, F. F., Alvalá, R. C., Mendes, R. M., & Amore, D. J. (2021). The influence of land use/land cover variability and rainfall intensity in triggering landslides: a back-analysis study via physically based models. *Natural Hazards*, 105(1), 1139–1161. doi:10.1007/s11069-020-04324-x.
- [51] Cantarino, I., Carrion, M. A., Goerlich, F., & Martínez Ibañez, V. (2019). A ROC analysis-based classification method for landslide susceptibility maps. *Landslides*, 16(2), 265–282. doi:10.1007/s10346-018-1063-4.
- [52] Yang, S., & Berdine, G. (2017). The receiver operating characteristic (ROC) curve. *The Southwest Respiratory and Critical Care Chronicles*, 5(19), 34. doi:10.12746/swrccc.v5i19.391.
- [53] SNI 8291. (2016). *Determination and Compilation of Landslide Zonation*. Badan Standardisasi Nasional, Jakarta, Indonesia. (In Indonesian).